Investigation of the Structural, Electrical, and Thermoelectric Characteristics of $XMnH_3$ (X = Na, K, and Rb) Perovskites Hydrogen Storage Using DFT

Youssef Jouad[1,2*], *Ayoub* Koufi[1,2], *Younes* Ziat [1,2], *Hamza* balkhanchi[1,2], *Noureddine* Lakouari[3], *Charaf* Laghlimi[4,2], *El Houssayne* Bougayr[5], *Hamid* Hamdani[1,2], *Issam* Forsal[5]

[1]Engineering and Applied Physics Team (EAPT), Superior School of Technology, Sultan Moulay Slimane University, Beni Mellal, Morocco
[2]The Moroccan Association of Sciences and Techniques for Sustainable Development (MASTSD), Beni Mellal, Morocco
[3]National Institute of Astrophysics, Optics and Electronics (INAOE), Puebla, Mexico. Secretariat of Science, Humanities, Technology and Innovation (Secihti), Mexico
[4]ERCI2A, FSTH, Abdelmalek Essaadi University, Tetouan, Morocco.
[5]Laboratory of Engineering and Applied Technologies, Higher School of Technology, Sultan Moulay Slimane University, Beni Mellal, Morocco

Abstract. In the present study, the structural, electrical, and thermoelectric properties of the perovskite hydrides $XMnH_3$ (X = Na, K, and Rb) were investigated using density functional theory (DFT) within the generalized gradient approximation (GGA). The calculations were performed using the Wien2k code, incorporating the BoltzTraP software package for thermoelectric analysis. The zero band gap and the overlap between the valence and conduction bands indicate metallic behavior in all compounds. The thermal conductivity of $NaMnH_3$, $KMnH_3$, and $RbMnH_3$ was found to increase with temperature. These results highlight the potential of $XMnH_3$ compounds for applications in thermoelectric devices and hydrogen storage, thereby contributing to the advancement of a sustainable hydrogen-based energy economy.

1 Introduction

Globally, hydrogen is gaining traction as one of the energy vectors to support the shift to a low-carbon, more sustainable economy [1]. It is an excellent way to help slow down climate change, as it doesn't release greenhouse gases when burned [2]. Although it is extremely common in the cosmos and the least dense chemical element, hydrogen is hardly ever seen in the physical world in its pure form [3]. It combines with oxygen in a fuel cell to generate electricity, with water vapor as a byproduct. This process is silent, clean, and incredibly effective [4]. However, despite these enormous benefits, hydrogen has many important

* Corresponding author: jouad.youssef@usms.ac.ma

technological limitations, namely in the areas of storage and transportation [5]. Due to its low energy density per volume, it cannot be effectively used unless it is compressed, liquefied, or stored in chemical bonds [6].

Particularly for bulk uses, like the transportation sectors (hydrogen-powered cars, aircraft, ships) or the production and storage of renewable energy, these processes are problematic in terms of technological complexity, expense, safety, and weight [7]. Therefore, the biggest scientific and technical barrier to rendering hydrogen competitively replaceable with fossil fuel is the development of new and effective storage material [8].

Perovskite materials have attracted considerable interest as potential alternatives for hydrogen storage due to their intriguing physicochemical properties. Their high surface area and porous structural nature facilitate efficient hydrogen adsorption and desorption, thereby enhancing storage capacity and kinetic performance. Additionally, many perovskites possess inherent catalytic properties that enable hydrogen evolution and uptake reactions, making them highly compatible with clean and sustainable energy systems. The flexibility of their general crystal structure, typically represented as ABX_3 where A and B are cations and X is usually a hydride or oxide anion allows for precise chemical tuning to optimize hydrogen absorption characteristics. In particular, perovskite hydrides have demonstrated significant potential for reversible hydrogen storage, offering both high gravimetric and volumetric capacities [9]. Furthermore, the properties of these materials can be tailored using advanced computational techniques, such as Density Functional Theory (DFT), which facilitate the prediction and optimization of their thermodynamic stability and hydrogen interaction behavior. Perovskite hydrides also support efficient photoelectrochemical and electrochemical reactions, enabling their seamless integration into hydrogen production, storage, and conversion systems. In addition, their intrinsic electronic and thermoelectric properties make them excellent candidates for multifunctional energy devices, which are essential for advancing sustainable and hydrogen-based energy technologies.

Thermoelectric technology offers considerable potential for achieving maximum performance in the direct conversion of heat into electricity, thus contributing to more efficient and environmentally friendly energy harvesting. With this in mind, perovskite-type hydrides stand out for their scalable electronic and thermoelectric properties, positioning them as promising candidates for high-density energy storage devices. In particular, the compounds $XMnH_3$ (where X = Na, K, Rb) are being extensively investigated for their thermoelectric properties, with the aid of ab initio calculations based on density functional theory (DFT), using the generalized gradient approximation (GGA) and BoltzTraP software. This approach enables key quantities such as the electrical conductivity, electronic thermal conductivity merit factor, and power factor to be accurately determined as a function of temperature. The main objective is to analyze how these properties contribute to the efficient conversion of thermal energy into electrical energy, thereby promoting the development of renewable energy technologies. Thanks to their metallic behavior, efficient electronic transport and structural stability at high temperatures, $XMnH_3$ compounds have great potential for integration into generators of renewable energy.

2 Calculation Method

In the present work, the storage capacity of hydrogen and essential physical properties of perovskite-type hydrides $XMnH_3$ (with X as Na, K, and Rb) were investigated systematically using first-principles calculations in Density Functional Theory (DFT). For a reliable description of the exchange–correlation interactions, Generalized Gradient Approximation (GGA) was applied a resulting in consistent and reliable computational results. The thermoelectric behaviors of the compounds were then examined using the WIEN2k code in conjunction with the BoltzTraP package[10, 11], which permits calculation of transport

coefficients from electronic band structures within the constant relaxation time approximation τ. These calculations provide details on parameters such as the electrical conductivity, and thermal conductivity requirements for assessing thermoelectric performance. For numerical accuracy and computational convergence, the self-consistent field (SCF) computations were strictly under a tight control, with thresholds for the convergence being set at 10^{-4} Ry for total energy and 10^{-3} electrons for charge density. High-density and uniform Brillouin zone sampling was achieved using a 10×10×10 k-point mesh to offer high accuracy in reciprocal-space integration. These research choices all lead to a complete and reliable evaluation of the electronic, structural, and thermoelectric features of the $XMnH_3$ compounds, which indicate their promise for hydrogen storage as well as energy-related applications.

To guarantee the precision of our DFT calculations, we conducted a systematic k-point convergence analysis for each of the three compounds examined in this study: $NaMnH_3$, $KMnH_3$, and $RbMnH_3$. The total energy for each system was calculated using progressively denser Monkhorst–Pack k-point meshes, varying from 3×3×3 to 12×12×12. The convergence findings are illustrated in Figures 1(a-c). The figures distinctly indicate that the total energy stabilizes for k-point grids equal to or beyond 8×8×8, with energy discrepancies of less than 0.001 Ry for denser meshes. Therefore, we used the 10×10×10 grid for the ensuing computations. This number offers an optimal equilibrium between numerical precision and computing efficiency. In the WIEN2k calculations, the plane-wave cutoff is determined by the product RMT × Kmax, rather than by an energy value in electron volts (eV). Here, RMT denotes the smallest muffin-tin radius (in atomic units, a.u.), while Kmax is the largest modulus of the reciprocal lattice vectors used in the plane-wave expansion of the interstitial wavefunctions. In this work, we employed the commonly accepted value of RMT × Kmax = 7.0, which is generally sufficient to achieve convergence in similar hydride perovskite systems. The muffin-tin radii (RMT) used for the $NaMnH_3$ compound were 2.20 a.u. for sodium, 2.19 a.u. for manganese, and 1.80 a.u. for hydrogen. For $KMnH_3$, the radii were 2.30 a.u. for potassium, 2.30 a.u. for manganese, and 1.28 a.u. for hydrogen. In the case of $RbMnH_3$, the chosen values were 2.30 a.u. for rubidium, 2.30 a.u. for manganese, and 1.33 a.u. for hydrogen.

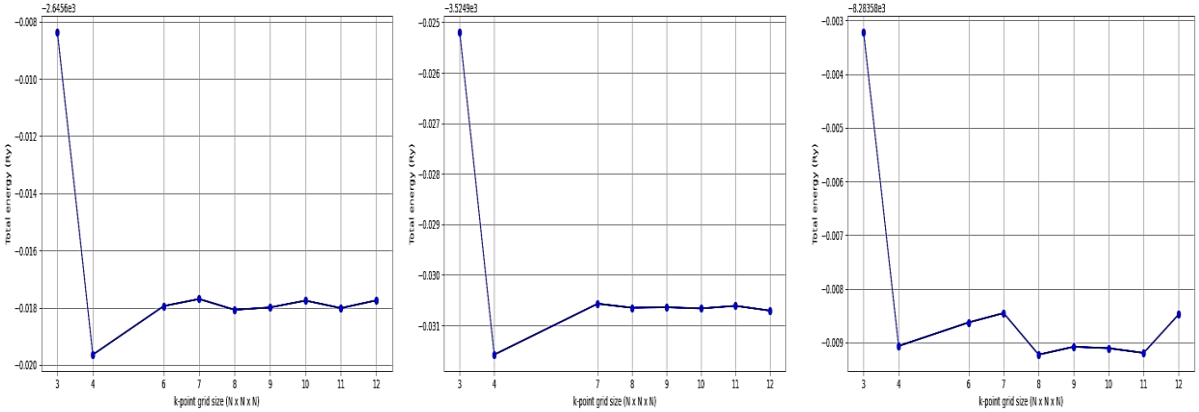

a) b) c)

Fig. 1. Convergence of Total Energy as a Function of k-point Mesh Size for $NaMnH_3$, $KMnH_3$, and $RbMnH_3$

3 Results and discussion

3.1 Structural properties

The crystal lattice structure shows how the atoms are arranged in the hydride perovskites $XMnH_3$ compounds, where X can be Na, K, or Rb. The disposition places the Mn atoms at the center (1/2, 1/2, 1/2) and the X atoms (Na, K, and Rb) at the corners (0, 0, 0). At the center of the faces are three hydrogen atoms located at the octahedral sites (0, 1/2, 1/2), (1/2, 0, 1/2), and (1/2, 1/2, 0). The structure is Pm-3m (No. 221) space group, with lattice parameters $a_0 = b_0 = c_0 = 3.59$ Å, 3.89 Å, and 4.05 Å, of $NaMnH_3$ $KMnH_3$ and $RbMnH_3$ respectively, with $\alpha = \beta = \gamma = 90°$, these values compare favorably with the Other work $a_0 = b_0 = c_0 = 3.59$ Å [12], 3.89 Å [12], and 4.05 Å [12], of $NaMnH_3$ $KMnH_3$ and $RbMnH_3$ respectively. This crystal structure is shown in Figure 2, which describes the periodicity of atoms and how they contribute to the formation of structural stability in $XMnH_3$ (X is Na, K, and Rb).

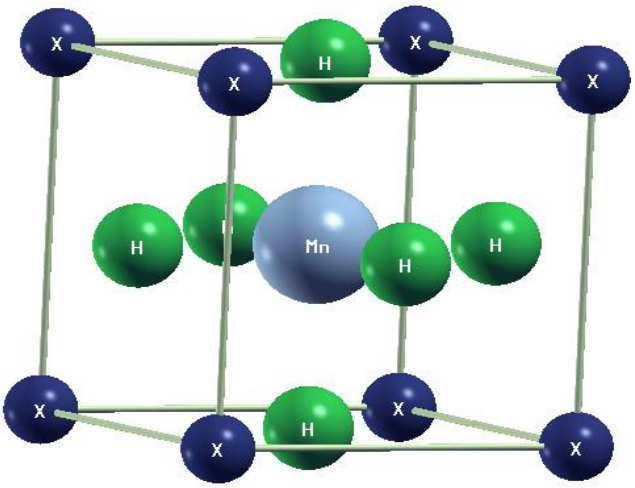

Fig. 2. Structure of *X*MnH_3 *(X = Na, K and Rb)*

3.2 Electronic properties

Within the framework of Density Functional Theory (DFT), the Generalized Gradient Approximation (GGA) [15] has been employed to calculate the electronic properties of the hydride perovskites $XMnH_3$, where X = Na, K, and Rb. Such computations are essential for understanding the electronic characteristics of these materials and evaluating their potential for practical applications. The band structures and density of states (DOS) of the compounds are illustrated in Figures 3 and 4. The observed overlap between the valence band maxima (VBM) and conduction band minima (CBM) at the Fermi level (E_x), located at 0 eV, clearly indicates a metallic character. This metallic nature is further confirmed by the partial density of states (PDOS) analysis presented in Figure 4. The VBM, in the energy range of -6 to -2.7 eV, is predominantly governed by the s orbitals of the X-site atoms (Na, K, and Rb), with notable contributions from the hydrogen s states. The metallic behavior of these compounds is attributed to the strong hybridization between the s states of the alkali metals (Na, K, Rb) and hydrogen. It is important to note that metallic materials, such as the perovskite hydrides investigated in this study, are highly suitable for hydrogen storage applications. Their

inherent electrical conductivity facilitates efficient charge transfer during hydrogen absorption and desorption processes [13]. Taken together, the analysis of the band structure and DOS confirms that $XMnH_3$ compounds exhibit metallic conductivity, making them promising candidates for industrial applications, particularly in hydrogen storage technologies [14].

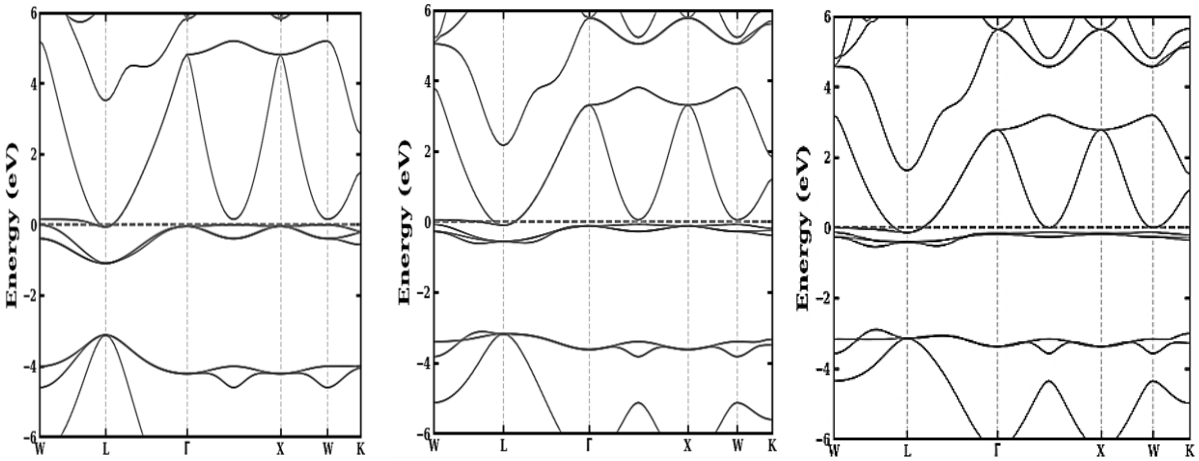

$NaMnH_3$ $KMnH_3$ $RbMnH_3$

Fig. 3. Band Structures of *X*MnH_3 *(X = Na, K and Rb)*

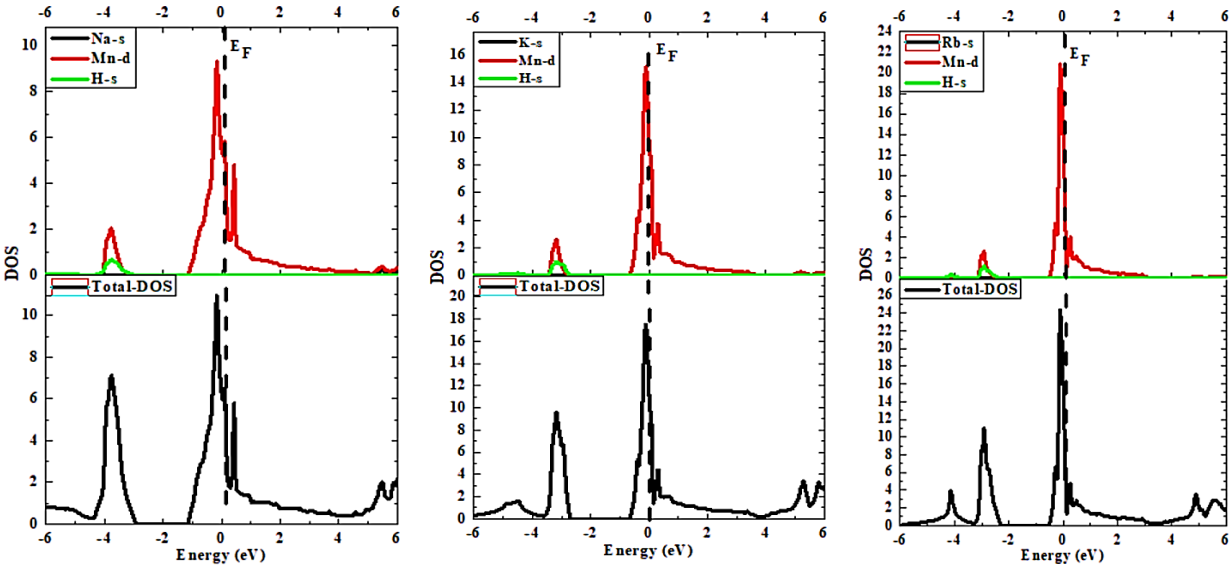

$NaMnH_3$ $KMnH_3$ $RbMnH_3$

Fig. 4. DOS of *X*MnH_3 *(X = Na, K and Rb)*

3.3 Thermoelectrical Properties

The thermoelectric property of $XMnH_3$ compounds with X = Na, K, and Rb is crucial for converting heat into electricity in renewable energy systems, where thermal energy frequently goes to waste. Electron transport behavior is essentially controlled by electron

band structure, which is computed using the Boltz-Trap code package. The investigation of these materials has been driven by the established functions of the electrical conductivity (σ/τ), and thermal conductivity (Kt), in controlling the material's merit factor (Zt), one of the main parameters used to describe the thermoelectric efficiency. The thermoelectric relationship between electrical conductivity and heat governing the operations of thermoelectric devices was studied between 300 K and 900 K temperatures. Zt, being a measure of the performance of the materials in terms of temperature, can be examined by taking the characteristic into account.

To determine the perovskite $XMnH_3$ viability for thermoelectric application, where X = Na, K, and Rb, one must decide on its electrical conductivity. Electric conductivity is described in terms of free charge carriers' mobility, which depends on many factors, including the crystal phase, defects or dopants within the crystal lattice, and composition of the material. Electrical conductivity and charge carrier mobility depend directly on these factors. Figure 5(a) indicates that the electrical conductivity of $NaMnH_3$ and $KMnH_3$ increases with temperature. But in $RbMnH_3$, electrical conductivity continues to increase from 500 K up to 900 K and decreases from 300 K to 500 K as temperature increases. The compounds depict varying behaviors because each element X (Na, K, and Rb) has a unique crystal structure and set of electrical interactions. Because of the temperature dependency of their electrical conductivity, such materials can function otherwise under varying conditions of application. Additionally, the electronic functionality of such materials may be affected by the test temperature and pressure, and this may impact electrical conductivity. Our study aims to ensure that adequate characterization is necessary to effectively utilize $XMnH_3$ material in thermoelectric devices, or even a device in general, where consistency and reliability of electrical conductivity are paramount.

In examining the performance of the material within thermoelectric devices, $XMnH_3$ (X = Na, K, and Rb) plays a crucial role since heat transport within the material is a function of its Kt. For the examined materials, thermal conductivity varies linearly with temperature (Figure 5(b)). The thermal conductivity values for $NaMnH_3$, $KMnH_3$, and $RbMnH_3$ at 900 K are $1.64*10^{15}$ W/(K.m.s), $1.225*10^{15}$ W/(K.m.s), and $1.43*10^{15}$ W/(K.m.s), respectively. The corresponding increase in thermal conductivity due to increasing temperature and increasing molecular vibrations is the reason for the respective increase in the case of $XMnH_3$ compounds. This has significance as this indicates that unreasonably high thermal conductivity will act against thermoelectric performance. For optimal functioning, thermoelectric devices based on $XMnH_3$ must balance thermal and electrical conductivity, although the latter is observed to increase with temperature. Variations among $NaMnH_3$, $KMnH_3$, and $RbMnH_3$ also show how changes in atomic composition influence the thermal behavior of these materials, suggesting that compound A might be carefully selected to offer optimal results for particular uses.

The following equation explains the **Zt**:

$$\mathbf{Zt} = \frac{\boldsymbol{\sigma S^2 T}}{\boldsymbol{\kappa}} \tag{1}$$

Zt variations for $XMnH_3$ (X = Na, K, and Rb) as a function of temperature can be seen in Figure 5(c). Zt for $RbMnH_3$ first decreases between 300 and 500 K, then increases between 500 and 900 K, reaching a value of $0.65*10^{-1}$ at 900 K. In contrast, Zt increases continuously with temperature for $NaMnH_3$ and $KMnH_3$. Despite being less effective at lower temperatures, this trend suggests that these materials grow dramatically with higher temperatures. In contrast, Zt increases gradually with temperature for $NaMnH_3$ and $KMnH_3$, reaching a peak at 900 K at $0.87*10^{-1}$ and $0.86*10^{-1}$, respectively.

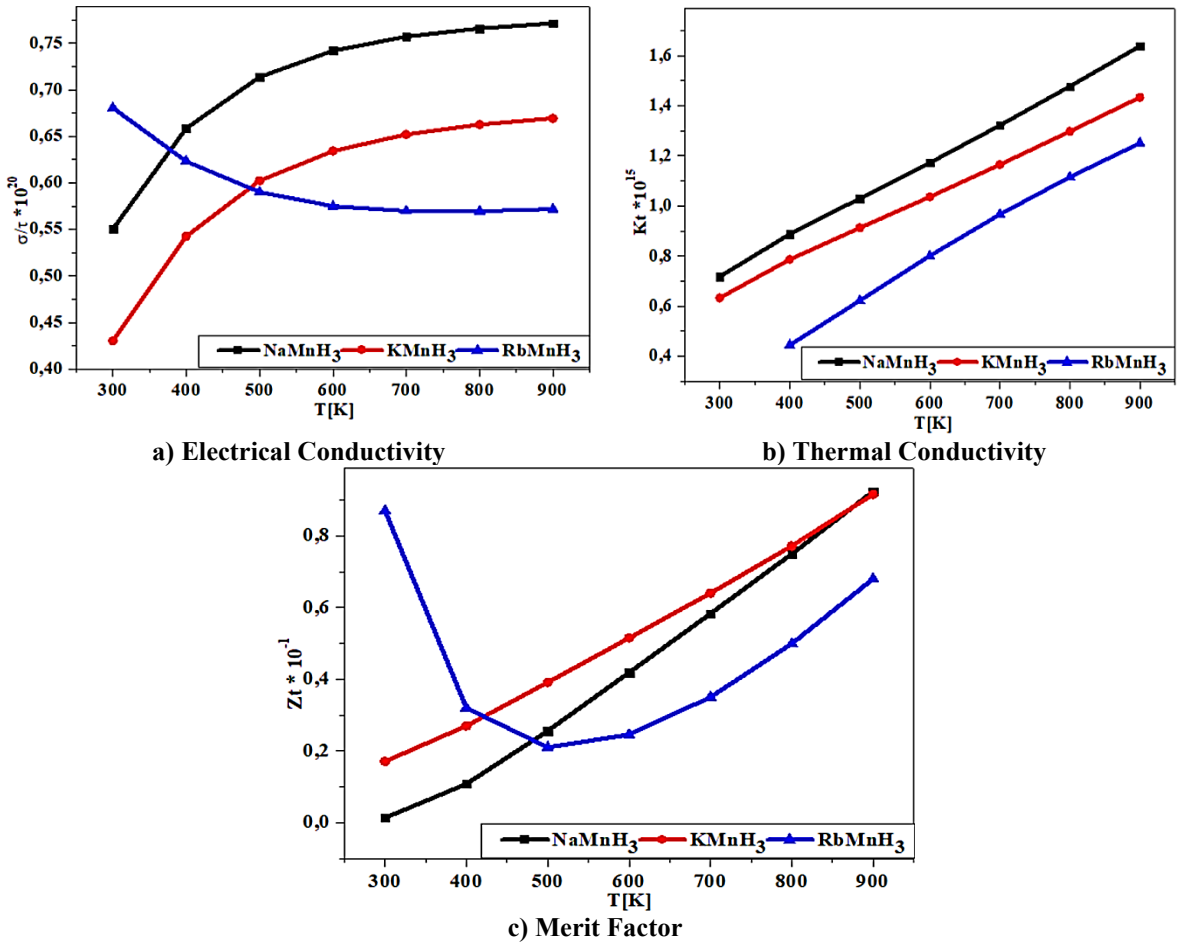

Fig. 5. Thermoelectric Properties of XMnH$_3$ *(X = Na, K and Rb)*

4 Conclusion

In conclusion, electrical, thermoelectric, and structural characteristics of XMnH$_3$, X=Na, K, and Rb hydride perovskite were computed using the Wien2k code and the BoltzTrap package. The outcome revealed that the compounds are conductors in nature, i.e., hydrogen storage compatibility. They possess an energy gap equal to 0 eV and overlapping valence and conduction bands. The values of merit factor (Zt), electrical conductivity, and thermal conductivity of the thermoelectric parameters demonstrated that NaMnH$_3$ and KMnH$_3$ are better than RbMnH$_3$ in all aspects of interest, especially at varying temperatures. Effective application of hydrogen storage technologies, supported by materials such as those described here, will be a significant stride toward a sustainable hydrogen economy, and this will make significant contributions to energy storage, transport, and industrial process applications. XMnH$_3$ (X is Na, K, and Rb) materials described here are of significant interest for numerous technological advances due to their unique characteristics developed for specific thermal conditions.

Funding: The authors are warmly grateful to the support of "The Moroccan Association of Sciences and Techniques for Sustainable Development (MASTSD), Beni Mellal, Morocco".

References

1. P. Mastropietro, & P. Rodilla. Support mechanisms for low-carbon hydrogen: The risks of segmenting a commodity market. Energy Policy, 202, 114605 (2025). https://doi.org/10.1016/j.enpol.2025.114605

2. D. J. Soeder. Greenhouse gas and climate change. In Energy futures: The story of fossil fuel, greenhouse gas, and climate change (pp. 97-141). Cham: Springer Nature Switzerland (2025). https://doi.org/10.1007/978-3-031-83603-9_5

3. C. Laghlimi, A. Moutcine, Y. Ziat, H. Belkhanchi, A. Koufi, S. Bouyassan, Hydrogen, chronology and electrochemical production. Sol. Energy Sustain. Dev. 14, 22–37 (2024). doi:10.51646/jsesd.v14iSI_MSMS2E.405

4. K. C. Mandal, T. Das, & B. K. Das. Nanomaterials for sustainable water splitting towards green hydrogen production. International Journal of Green Energy, 1-26, (2025). https://doi.org/10.1080/15435075.2024.2428365

5. X. Liu, Y. Huang, X. Shi, W. Bai, S. Li. P. Huang, ... & Y. Li. Offshore Wind Power Seawater Electrolysis Salt Cavern Hydrogen Storage Coupling System: Potential and Challenges. Energies, 18(1), 169 (2025). https://doi.org/10.3390/en18010169

6. E. Nemukula, C. B. Mtshali, & F. Nemangwele. Metal Hydrides for Sustainable Hydrogen Storage: A Review. International Journal of Energy Research, 2025(1), 6300225 (2025). https://doi.org/10.1155/er/6300225

7. S. A. Ali, I. A. Bangash, H. Sajjad, M. A. Karim, F. Ahmad, M. Ahmad, ... & A. Qudoos. Review on the Role of Electrofuels in Decarbonizing Hard-to-Abate Transportation Sectors: Advances, Challenges, and Future Directions. Energy & Fuels (2025). https://doi.org/10.1021/acs.energyfuels.4c06185

8. X. Pan, H. Zhou, D. Baimbetov, S. Syrlybekkyzy, S. B. Akhmetov, & Q. Abbas. Development Status and Future Prospects of Hydrogen Energy Technology: Production, Storage, and Cost Analysis. Advanced Energy and Sustainability Research, 2400451 (2025). https://doi.org/10.1002/aesr.202400451

9. A. Koufi, Y. Ziat, & H. Belkhanchi. Study of the Gravimetric, Electronic and Thermoelectric Properties of XAlH3 (X= Be, Na, K) as hydrogen storage perovskite using DFT and the BoltzTrap Software Package., Solar Energy and Sustainable Development, 53-66. (2024). https://doi.org/10.51646/jsesd.v14iSI_MSMS2E.403

10. P. Blaha, K. Schwarz, F. Tran, R. Laskowski, G. K. Madsen, & L. D. Marks. WIEN2k: An APW+ lo program for calculating the properties of solids. The Journal of chemical physics, 152(7). (2020)., https://doi.org/10.1063/1.5143061.

11. J. P. Perdew, K. Burke, M. Ernzerhof. Generalized gradient approximation made simple. Phys. Rev. Lett. 1996, 77(18), 3865. https://doi.org/10.1103/PhysRevLett.77.3865..

12. R. Song, N. Xu, Y. Chen, S. Chen, W. Dai, & W. Zhang. First-principles investigation for the hydrogen storage, mechanical, electronic, optical, dynamic, and thermodynamic properties of XMnH3 (X= Na, K, Rb), perovskites for hydrogen storage

applications. Vacuum, 222, 113007. (2024). https://doi.org/10.1016/j.vacuum.2024.113007

13. A. Siddique, A. Khalil, B. S. Almutairi, M. B. Tahir, M. Sagir, Z. Ullah, ... & M. Alzaid. Structures and hydrogen storage properties of AeVH3 (Ae= Be, Mg, Ca, Sr) perovskite hydrides by DFT calculations., International Journal of Hydrogen Energy, 48(63), 24401-24411. (2023). https://doi.org/10.1016/j.ijhydene.2023.03.139

14. B. P. Tarasov, P. V. Fursikov, A. A. Volodin, M. S. Bocharnikov, Y. Y. Shimkus, A. M. Kashin, ... & M. V. Lototskyy. Metal hydride hydrogen storage and compression systems for energy storage technologies., International Journal of Hydrogen Energy, 46(25), 13647-13657. (2021). https://doi.org/10.1016/j.ijhydene.2020.07.085

15. Y. Ziat, H. Belkhanchi, Z. Zarhri, DFT analysis of structural, electrical, and optical properties of S, Si, and F-doped GeO_2 rutile: implications for UV-transparent conductors and photodetection. Sol. Energy Sustain. Dev. 14, 74–89 (2025). https://doi.org/10.51646/jsesd.v14i1.232